Available online at www.sciencedirect.com

ScienceDirect

CAAI Transactions on Intelligence Technology 1 (2016) 259–271
http://www.journals.elsevier.com/caai-transactions-on-intelligence-technology/

Original Article

Unknown constrained mechanisms operation based on dynamic interactive control☆

Hesheng Wang [a,b,c], Bohan Yang [a,b], Weidong Chen [a,b,*]

[a] Department of Automation, Shanghai Jiao Tong University, Shanghai 200240, China
[b] Key Laboratory of System Control and Information Processing, Ministry of Education of China, China
[c] State Key Laboratory of Robotics and System, Harbin Institute of Technology (HIT), Harbin 150001, China

Available online 20 October 2016

Abstract

In order to operate various constrained mechanisms with assistive robot manipulators, an interactive control algorithm is proposed in this paper. This method decouples motion and force control in the constrained frame, and modifies the motion velocity online. Firstly, the constrained frame is determined online according to previous motion direction; then the selection matrix is adjusted dynamically, the constrained motion direction is chosen as the driving-axis. Consequently, the driving-axis and non-driving-axis are decoupled; finally, velocity control and impedance control are implied on above axes respectively. The selecting threshold for driving-axis is also varying dynamically to fit different constrained mechanism. Door-opening experiments are conducted to verify the performance of the proposed method.

Keywords: Unknown constrained mechanism; Selection matrix; Constrained frame; Robot manipulator; Impedance control

1. Introduction

The application field of the assistive robot is getting increasingly wide, and the interactions between assistive robot manipulators and the environment, such as opening the door, pulling a drawer, serving the tea, is becoming more and more closely [1–3]. There are various constrained mechanisms in the interactive environment. In the situations where task descriptions of each constrained mechanism are not necessary, manipulators need a way to operate the unknown constrained mechanisms.

The operation of unknown constrained mechanisms is very complicated. For instance, opening the door, which involves a series of problems such as positioning, trajectory planning, and tracking, is a typical problem of the unknown constrained mechanism operation. Most of the traditional opening-door operation needs to model the door first to plan a trajectory, which does not provide the universal solution because different tasks need different task descriptions. For example, Nagatani modeled the door and presented a detailed analysis of the path planning to open the door [4,5]; Peterson used the smallest-model analysis to predict the parameters but the success rate of opening the door is 90% [6]; Pujas proposed a force-position hybrid control method, but the inaccurate task description model might result in positioning errors [7]; Petrovskaya adopted the laser-scanning modeling based particle filter method which also suffered from the defects of inaccuracy [8]. There are also model-free methods. Schmid installed multi-point haptic sensors on the hand claw and force/torque sensors on the wrist to open the door operation, but this kind of method increased the complexity of the controller [9]; Lutscher proposed to operate the unknown constrained mechanisms based on

☆ This work was supported in part by the National Natural Science Foundation of China under Grant 61473191, 61503245, 61221003, in part by the Science and Technology Commission of Shanghai Municipality under Grant 15111104802, in part by State Key Laboratory of Robotics and System (HIT).

* Corresponding author. Department of Automation, Shanghai Jiao Tong University, Shanghai 200240, China.
E-mail addresses: wanghesheng@sjtu.edu.cn (H. Wang), wdchen@sjtu.edu.cn (W. Chen).

Peer review under responsibility of Chongqing University of Technology.

http://dx.doi.org/10.1016/j.trit.2016.10.004

an impedance control method, which adjusted the guiding speed by impedance control to achieve two-dimensional plane operation [10]; On the basis of [10], we put forward a operation method based on impedance control and the motion prediction. By fitting the historical trajectory to estimate motion model, and then adjusting the orientation and amplitude of the guiding speed, the operating efficiency is improved [11]; Furthermore, we put forward the dynamic hybrid complaint control method [12] that online chooses traction axis and estimates constraint coordinate system. Besides, the operating space is not limited by the two-dimensional plane. However, because the threshold of the traction axis selection is fixed, this method cannot manipulate constrained mechanisms with different resistance.

This paper proposed a dynamic interacting control based method, which developed from the force/position hybrid control [13] that introduces dynamic selection matrix to dynamically choose the direction of the force and speed control. Besides, this method does not require a detailed task description. The constrained motion direction is chosen as the driving axis, and other axes as the non-driving axis. The speed-control method is adopted on the driving axis to produce active-traction effect, while the force-control method is used on the non-driving axis to adjust the position and posture of manipulator passively. Selection of the driving axis is the key point of this method. Under the precondition of the unknown constrained mechanisms moving direction, the driving axis can be selected randomly to test the moving direction of the constrained mechanisms. By selecting matrix criterion, the driving axis can be adjusted dynamically until the constrained mechanisms began to move. Then according to the moving direction of the constrained mechanisms, the dynamic constraint coordinate system can be dynamically estimated. And the decoupling of the driving axis and non-driving axis can be accomplished through the dynamic selection matrix. Through the dynamic adjustment, choose suitable driving axis is chosen to manipulate the unknown constrained mechanisms. Impedance control method is adopted on the non-driving axis, because the manipulators are moving follow the constrained mechanisms, which resulting in the position errors and the force errors. So force control alone cannot tracking the position errors of the manipulators in time. Impedance control does not directly control the desired force and position, but achieves the complaint function by controlling the dynamic relationship between position and force, which is suitable for the non-driving axis control method in this paper.

2. Controller design

This paper takes the door-opening task as an instance to introduce the dynamic interaction control based method to manipulate the on of the limited operation method to manipulate the unknown constrained mechanisms. It is assumed that the position and orientation of the door and the position of the door's axis are unknown. For simplicity, it is assumed that the end effector has grasped the doorknob as shown in Fig. 1. As shown in the figure, the robot's base frame is denoted as $\sum_b$, the end-effector frame is denoted as $\sum_e$, and the constrained frame is

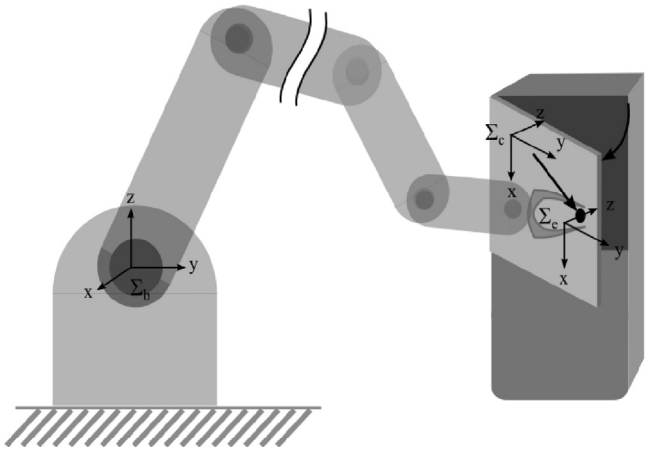

Fig. 1. The system model.

denoted as $\sum_c$. The origins of $\sum_c$ and $\sum_e$ are of coincidence, which are both the doorknob denoted by p_c with respect to $\sum_b$.

2.1. Control system design

The block diagram of the control system is shown in Fig. 2. The system can be mainly divided into operating space velocity controller and the angular velocity controller. The outputs of the linear velocity controller and the angular velocity controller are add together to produce the control velocity, after that it will be transferred to the joint space through the differential inverse kinematics. The linear velocity controller adopts the dynamic interactive control method and the angular velocity controller adopts the moment-following control method.

Under $\sum_c$, assume that $\dot{p}^c$ is the current linear velocity, $\dot{p}_d^c$ is the desired linear velocity, ω is the control angular velocity, ω is the linear velocity of the end effector, v_i is the driving linear velocity, f_d^c is the desired control force, τ_d^c is the desired control torque, $\dot{p}$ is the control velocity of the end effector. $R_e^c(v^e)$ is the rotation matrix from the end-effector frame to the constrained frame, $v^e = (v_x, v_y, v_z)$ is the end effector's velocity with respect to the end-effector frame, S is the selection matrix. The force and torque measured under $\sum_e$ by the six-dimension force/torque sensor are transferred to the constrained frame $\sum_c$ and denoted as h^c, including force f^c and torque τ^c.

As shown in the Fig. 2, $R_e^c(v^e)$ and S are changed dynamically. The former selects the dynamic constrained frame and the latter selects the driving axis, which will described in Section 2.2. Because the constrained mechanism is unknown, $\dot{p}_d^c$ is unknown. In the k th control period, define the desired velocity of the $k+1$ th control period as:

$$\dot{p}_d^c(k+1) = \dot{p}^c(k) \tag{1}$$

The control steps are as follows:

1) Give an arbitrary initial speed to the end effector to test the movement;
2) According to the moving direction of the constrained mechanisms, the constrained frame and the selection matrix are dynamically chosen;

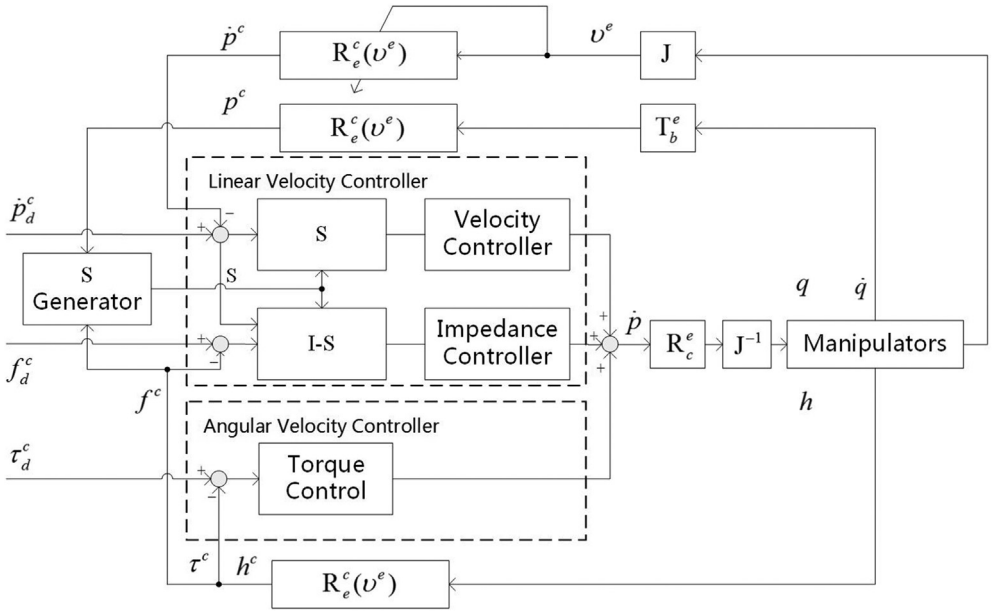

Fig. 2. Block diagram of the control system.

3) Define the driving axis through the dynamic selection matrix, and decouple the driving axis and the non-driving axis, then apply a constant driving velocity on the driving axis while apply the impedance control on the non-driving axis to adjust the manipulator's position and orientation;
4) Repeat from step 2).

2.2. Linear velocity controller

Because the model of the constrained mechanism is unknown, the desired trajectory of the manipulator cannot be defined in advance. If the general force/position hybrid control method is adopted, a detailed task description is necessary [13]. In order to avoid the task description and improve the applicability of the operation, this paper proposes a dynamic interactive control based operating method that online estimates the operating direction.

The core idea of this article includes the online estimation of the dynamic constrained frame, the determination of the dynamic selection matrix and the design of the velocity controller. The dynamic constrained frame and the dynamic selection matrix are used to determine the driving axis and the non-driving axis.

2.2.1. Online regulation of the constrained frame

As shown in Fig. 3, the arc is the constrained trajectory of the constrained mechanism. $\sum_e$ is the end effector frame, $\sum_c$ is the constrained frame. The origins of $\sum_c$ and $\sum_e$ are of coincidence, which are both the doorknob denoted by p_c with respect to $\sum_b$. $\sum_e$ is known, while $\sum_c$ is unknown.

During the movement of the constrained mechanism, the actual moving direction is the same with the constrained moving direction. According to this, the constrained moving direction is chosen as the driving axis to make the constrained mechanism moving along the correct direction. The driving axis is chosen under the constrained frame, therefore the estimation of the constrained frame is particularly important.

The constrained frame at time k + 1 is estimated according to the constrained moving directions at time k-1 and time k. As shown in Fig. 3, the z axis of the constrained frame is parallel with the tangent of the constrained trajectory because the tangent direction is the constrained moving direction. Under $\sum_c$, determine the z axis as the driving axis through the selection matrix S, which will be introduced later. Under $\sum_e$, the end effector velocity at time k is $v^e = (v_x, v_y, v_z)$, and the constrained direction is,

$$d_k = \left(\frac{v_{xk}}{\sqrt{v_{xk}^2 + v_{yk}^2 + v_{zk}^2}} \quad \frac{v_{yk}}{\sqrt{v_{xk}^2 + v_{yk}^2 + v_{zk}^2}} \quad \frac{v_{yk}}{\sqrt{v_{xk}^2 + v_{yk}^2 + v_{zk}^2}} \right)$$

The constrained moving direction d_k is the unit vector of the Z axis with respect to $\sum_e$. Similarly, the direction of time k-1 is represented by a unit vector $d_{k\text{-}1}$. During the two adjacent control period, the end effector is moving in the same plane. Thus the X axis of the constrained frame is perpendicular with the plane defined by d_k and $d_{k\text{-}1}$. And the unit vector of the X axis with respect to the end effector is:

$$d_{xk} = \frac{d_{k-1} \times d_k}{\| d_{k-1} \times d_k \|}$$

According to the right-hand rule, the Y axis of the constrained frame can be determined. Then the end rotation matrix R_e^c between the end effector frame and the constrained frame can be calculated.

2.2.2. Dynamic estimation of the selection matrix

This paper adopts a force/position hybrid control method to manipulate the constrained mechanism. During this process, use the dynamic selection matrix S to decouple the velocity

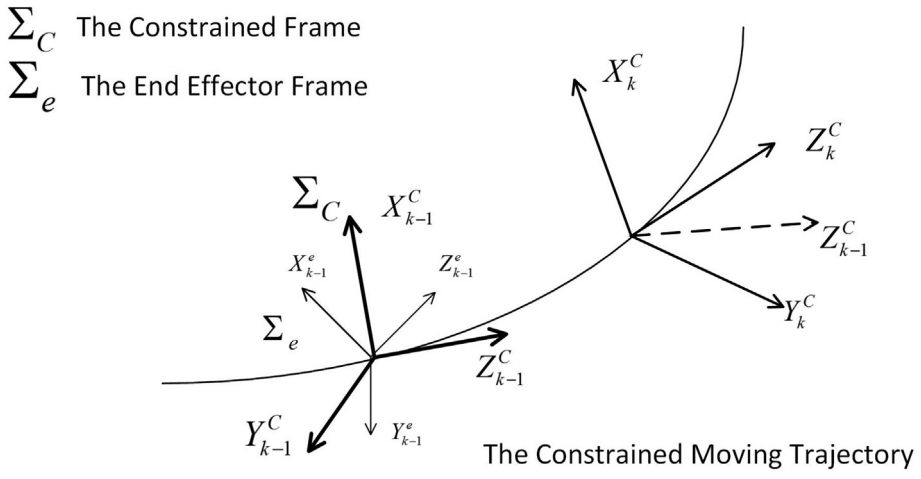

Fig. 3. The coordinate frames of end-effector and the constrained frame.

control and the force control. The element of S is 0 or ± 1, which is used to determine the control mode in each subspace. The elements ± 1 represent that the axis is chosen as the driving axis, and the sign stands for positive/negative direction. And the element 0 represents that the axis is chosen as the non-driving axis. In the direction selected by S, the current velocity $\dot{p}^c$ should track the desired velocity $\dot{p}_d^c$. And in the direction selected by I−S, the measured force f^c should track the desired force f_d^c. In this paper, the selection matrix S is a diagonal matrix with the dimension of 3, which can be designed as:

$$S = \begin{bmatrix} S_1 & & \\ & S_2 & \\ & & S_3 \end{bmatrix} \tag{2}$$

Its elements dynamically changes according to the force and position situation, and an arbitrary direction can be chosen as the initial direction of the driving axis. As long as the driving speed is applied on the axis direction with reasonable force and is capable of driving the constrained mechanism, the constrained mechanism can reach the actual moving trajectory. Thus the amplitude of force and the position error are regarded as judgments of the S generator:

$$S_1 = \begin{cases} 0 & (S_i = \pm 1, i \neq 1) \\ 1 & (f_x^c < \gamma, and \| \Delta p^c \| > 0 \\ & and\ S_i = 0, i \neq 1) \\ -1 & (f_x^c > \gamma, and \| \Delta p^c \| > 0 \\ & and\ S_i = 0, i \neq 1) \end{cases}$$

$$S_2 = \begin{cases} 0 & (S_i = \pm 1, i \neq 2) \\ 1 & (f_y^c < \gamma, and \| \Delta p^c \| > 0 \\ & and\ S_i = 0, i \neq 2) \\ -1 & (f_y^c > \gamma, and \| \Delta p^c \| > 0 \\ & and\ S_i = 0, i \neq 2) \end{cases} \tag{3}$$

$$S_3 = \begin{cases} 0 & (S_i = \pm 1, i \neq 3) \\ 1 & (f_z^c < \gamma, and \| \Delta p^c \| > 0 \\ & and\ S_i = 0, i \neq 3) \\ -1 & (f_z^c > \gamma, and \| \Delta p^c \| > 0 \\ & and\ S_i = 0, i \neq 3) \end{cases}$$

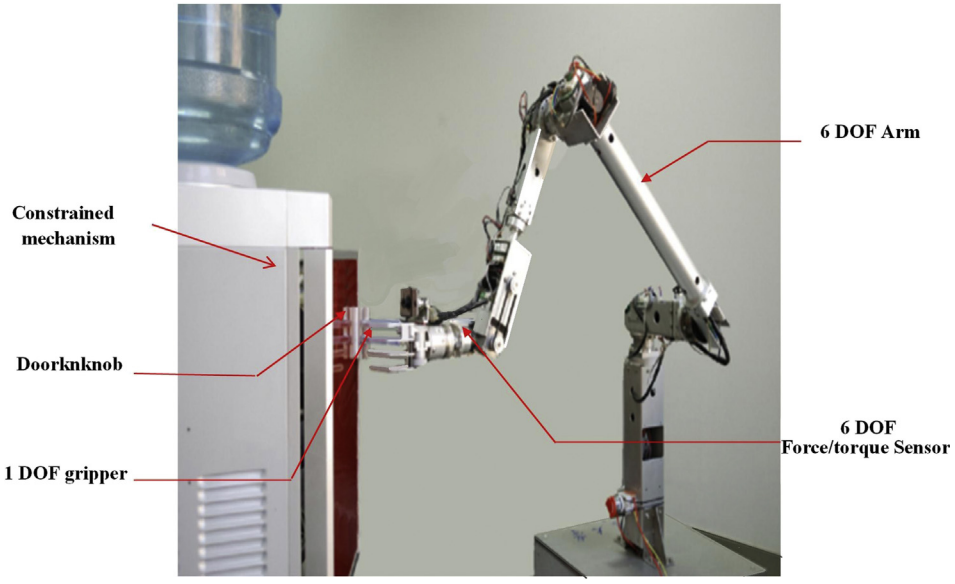

Fig. 4. The experiment setup.

Where γ is the threshold of the selection and δ is the threshold of the position error. These 3 judgments work in a cycle. At each time, only one axis is chosen as the driving axis. When the force on the driving axis becomes greater than the threshold or when the change of position along this direction is rather small, the element 1 in the matrix S should be replaced by -1; If the force and position error in the opposite direction fail to meet the requirements, then it is assume that this driving axis is not correct and other direction should be chosen. In this paper, the selection of the driving axis follows the x-y-z-x…cycle.

On the basis of [12], this paper adds a dynamic law to choose the threshold value γ to make the manipulator adapt to the constrained mechanisms with different resistance. Different constrained mechanisms have different operation resistance, a fixed threshold can only operate the constrained mechanisms whose resistance is within some threshold span, and cannot adapt to the mechanism with bigger resistance. While the dynamic threshold selecting law selects the threshold according to the number of judging cycles to dynamically adjust the value:

$$\gamma = \gamma_0 + \left[S_1\ f_x + S_2\ f_y + S_3\ f_z\right] \cdot L \tag{4}$$

Where γ_0 is the initial selecting value; [] is the integer notation that is used for get the integral value of the force on the driving axis; Only one of S_1,S_2,S_3 is zero in the door-opening process to make sure that $S_1 \cdot f_x + S_2 \cdot f_y + S_3 \cdot f_z$ is the force on the driving axis; L is the period of the judging cycle.

2.2.3. Controller design

After determining the constrained frame and the dynamic selection matrix, the velocity controller needs to be designed. Operate velocity control on the driving axis to give the axis a constant driving speed v_i; Operate impedance control on the non-driving axis to adjust the force error and position error on the axis.

Impedance control is an active complaint control method with the mass-spring character, which can relate force and position. This paper only considers the relationship of force errors and position errors on the non-driving axis. Under $\sum_c$, the translational mechanical impedance relationship between the position error on the non-driving axis $\Delta p^c = p^c - p_d^c$ and the force error on the non-driving force $\Delta f^c = f^c - f_d^c$ can be represents as follows [14]:

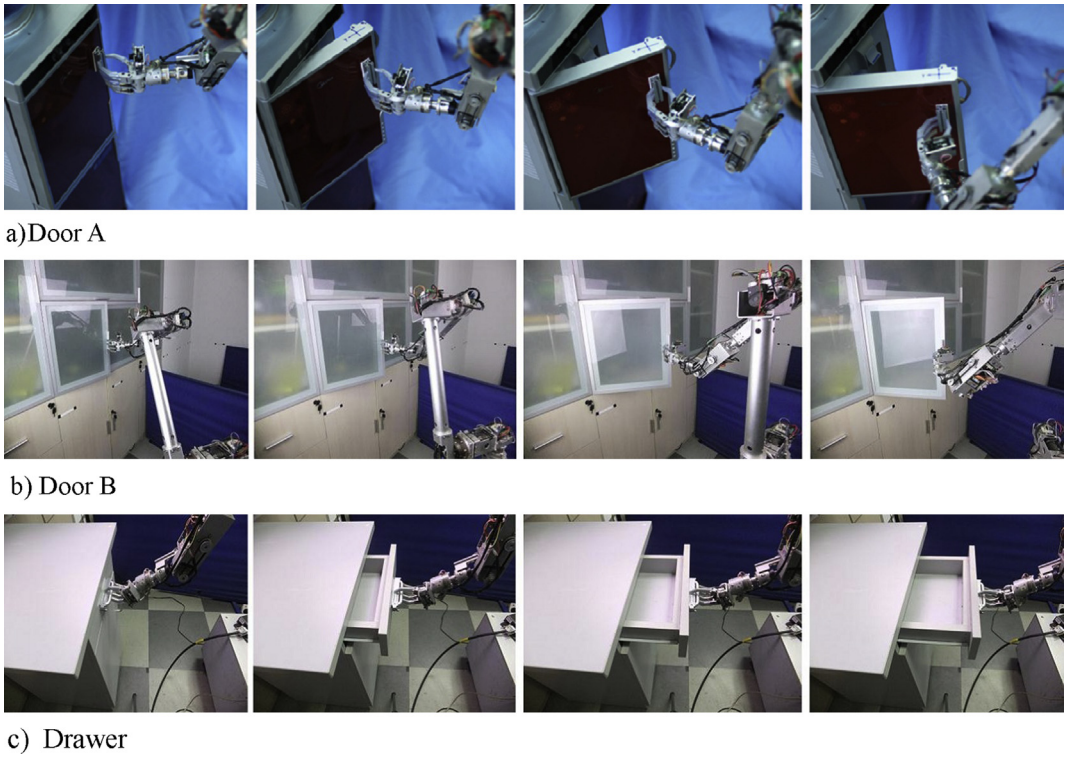

Fig. 5. Process of the autonomous operation.

Table 1
Comparison of experiments.

No.	Operation target	Motion Type	Algorithm	selection threshold γ	Intial Velocity	Driving Axis	Dynamic Velocity
Exp. I	door A	Circular motion	Impedance control [11]	Fixed	(0,vsin(π/4),vcos(π/4))	X	No
Exp. II	door A	Circular motion	Dynamic Interactive Control	Fixed	(0,vsin(π/4),vcos(π/4))	X	No
Exp. III	door A	Circular motion	Dynamic Interactive Control	Fixed	(0,vsin(π/4),vcos(π/4))	X	Yes
Exp. IV	door B	Circular motion	Dynamic Interactive Control	Dyanmic	(0,vsin(π/4),vcos(π/4))	X	Yes
Exp. V	drawer	Linear motion	Dynamic Interactive Control	Dyanmic	(0,vsin(π/4),vcos(π/4))	X	Yes

$$\Delta f^c = M \cdot \Delta \ddot{p}^c + D \cdot \Delta \dot{p}^c + K \cdot \Delta p^c \quad (5)$$

Where M, D, K are 3 × 3 matrix that represents the inertia matrix, damping matrix and stiffness matrix respectively. On the non-driving axis, the input force Δf^c can result in position changes, which in turn will lead to the decrease of the force Δf^c. Δp^c can be calculated by (5). According to [14], we have:

$$p^c(k) = p_d^c(k) + \Delta p^c(k) \quad (6)$$

Calculate the derivation of both side of (6), and according to (1), we have:

$$\dot{p}^c(k) = \dot{p}^c(k-1) + \Delta \dot{p}^c(k)$$

Using the dynamic rotation matrix R_e^c of the constrained frame determined before, the control velocity under $\sum_c$ can be calculated as:

$$v' = S \cdot v_i + (I - S) \cdot \dot{p}^c$$

Because the speed is constant, relatively large force error might occur at the beginning of the test of the operating direction and the test time is relatively long. In order to decreasing the force error and speeding up the test, a speed-change controller is proposed to dynamically adjust the speed according to the change of the force on the driving axis during the door-open process [11]:

$$v = V \cdot \frac{v'}{\|v'\|} \quad (7)$$

Where V is the desired speed that can be calculated as:

$$V = V_{\max} \cdot e^{-\varepsilon \left| S_1 \ f_x + S_2 \ f_y + S_3 \ f_z \right|}$$

Where V_{max} is the threshold of V, which is adjustable; The gain coefficient ε is positive and used to control the speed of V's variation; Only one of S_1,S_2,S_3 is zero in the door-opening process to make sure that V changes follow the change of the force on the driving axis.

2.3. Angular velocity controller

Angular velocity controller uses impedance control of position and orientation to determine the angular velocity of the end effector to adjust its position and orientation. Under the constrained frame, the relationship between the end effector's angular velocity ω and torque τ^c is as follows:

$$\tau^c = M_{rot} \cdot \dot{\omega} + D_{rot} \cdot \omega \quad (8)$$

Where M_{rot}'D_{rot} are 3 × 3 matrix that represents the inertia matrix, damping matrix in the impedance control respectively. The end effector's angular velocity ω can be calculated through (8).

According to (7) and (8), the control velocity can be obtained:

$$\dot{p} = \begin{bmatrix} v \\ \omega \end{bmatrix}$$

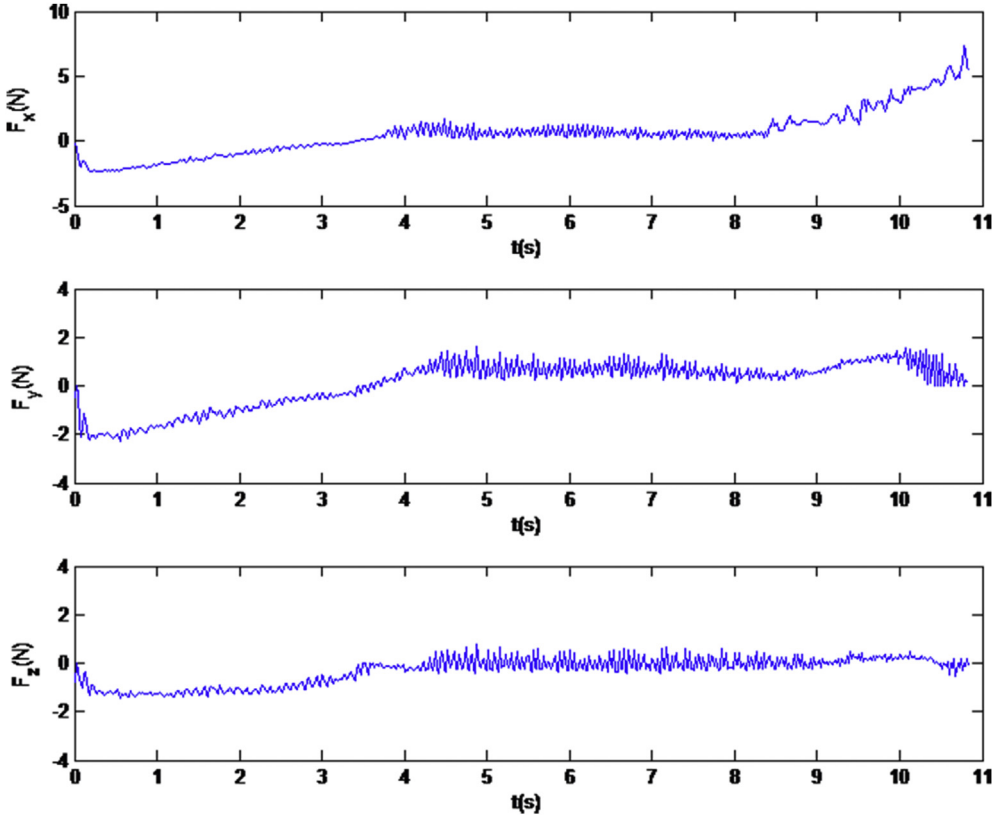

Fig. 6. Force response curve of Exp. I.

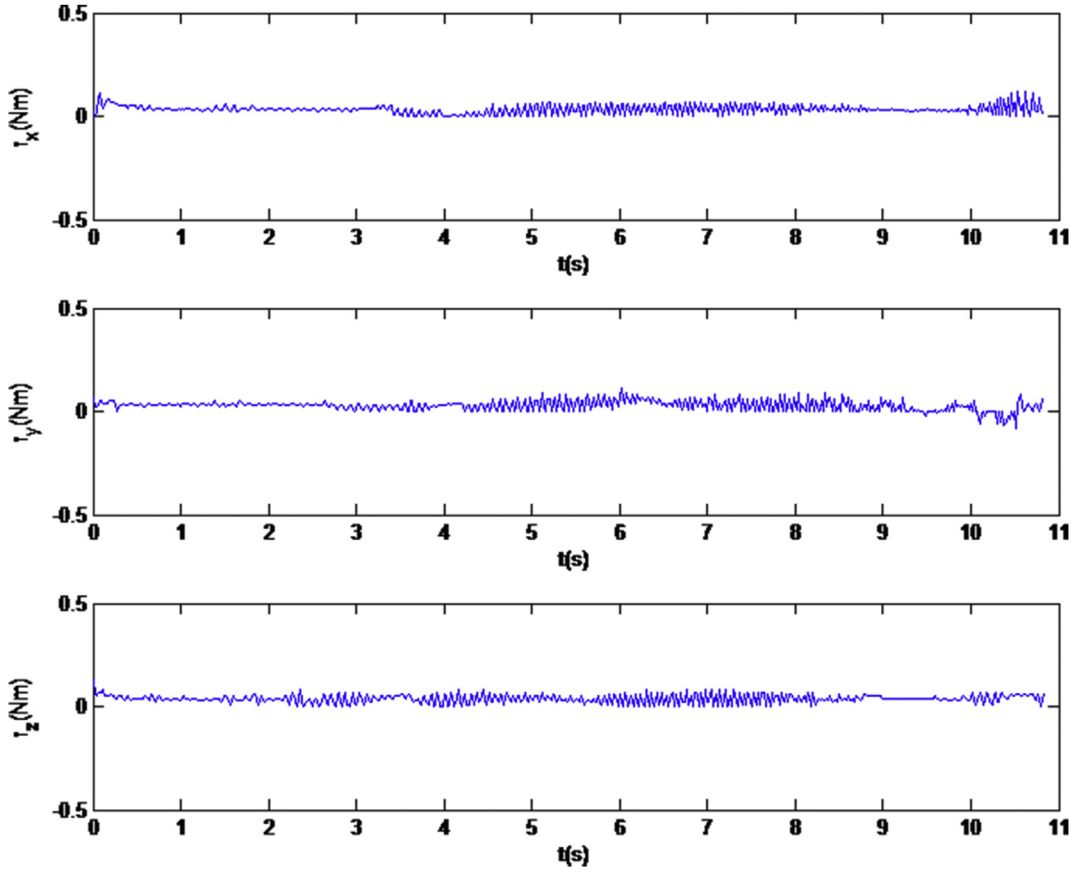

Fig. 7. Torque response curve of Exp. I.

It can be transferred to the joint space to input to the manipulators by the inverse differential kinematics.

3. Experiments and analysis

3.1. Experimental systems

To verify the effectiveness of the proposed method, a series of experiments on operating constrained mechanism are conducted. The experimental system is shown in Fig. 4. In this study, a 6-DOF robot manipulator [11,15] developed by autonomous laboratory of Shanghai Jiao Tong University. A 1 DOF gripper is equipped. Forces and moments are obtained through the six-axis force/torque sensor of ATI's Mini45 mounted on the wrist of the manipulator. An Inter Core 2 computer with windows operating system is adopted as the main controller. The main control cycle is 20 ms.

3.2. Experimental systems

Five experiments have been conducted in this paper. A traditional Impedance control method [11] is adopted in Experiment I. Experiment II, III, IV and V are based on the dynamic interactive control method proposed in this paper. A dynamic velocity method is involved in Experiment III, Iv and V. The operation target of Experiment I, II and III is door A. The selection threshold is estimated dynamically to operate door B in Experiment IV and to operate drawer in Experiment V. The Process of the autonomous operation are shown in Fig. 5, Table 1 lists the experimental contrast details.

In Experiment I and II, v is equal to 10 mm/s. In Experiment II and III, the selection threshold is set as γ=1.5N based on experience. In Experiment III, IV and V, dynamic velocity method is adopted with V_{max} = 15 mm/s, ε=2.0. The selection threshold is estimated dynamically in Experiment IV with γ_0 = 1.5 N, The initial value of L is 0. In these experiments, the coordinate frame of the end-effector and the door are parallel to each other. The initial speed are (0,$v\sin\theta$,$v\cos\theta$) in $\sum_c$, θ=π/4. The initial driving axis is the X axis.

Assume the motion speed of the arm during door opening is not big. The effects of M and D in the impedance control are ignored and only K item is considered, whose diagonal elements are set to 4.0 N/mm. The effects of M_{rot} in attitude impedance control is also negligible. The attitude of the doorknob need by followed by the end-effector of the arm real-time, K_{rot} is set to zero. Only the item D_{rot} is left, all the diagonal elements are set as 1.9 Nms/rad.

In these experiments, all operation tasks have been successfully completed by the robot arm. These response contact forces and moments of the end-effector are shown in Figs. 6–14. Detail analysis are discussed as follows.

The effectiveness of the proposed dynamic interactive control algorithm and the influence of dynamic dajustment of the velocity are demonstrated in Experiment I, II and III.

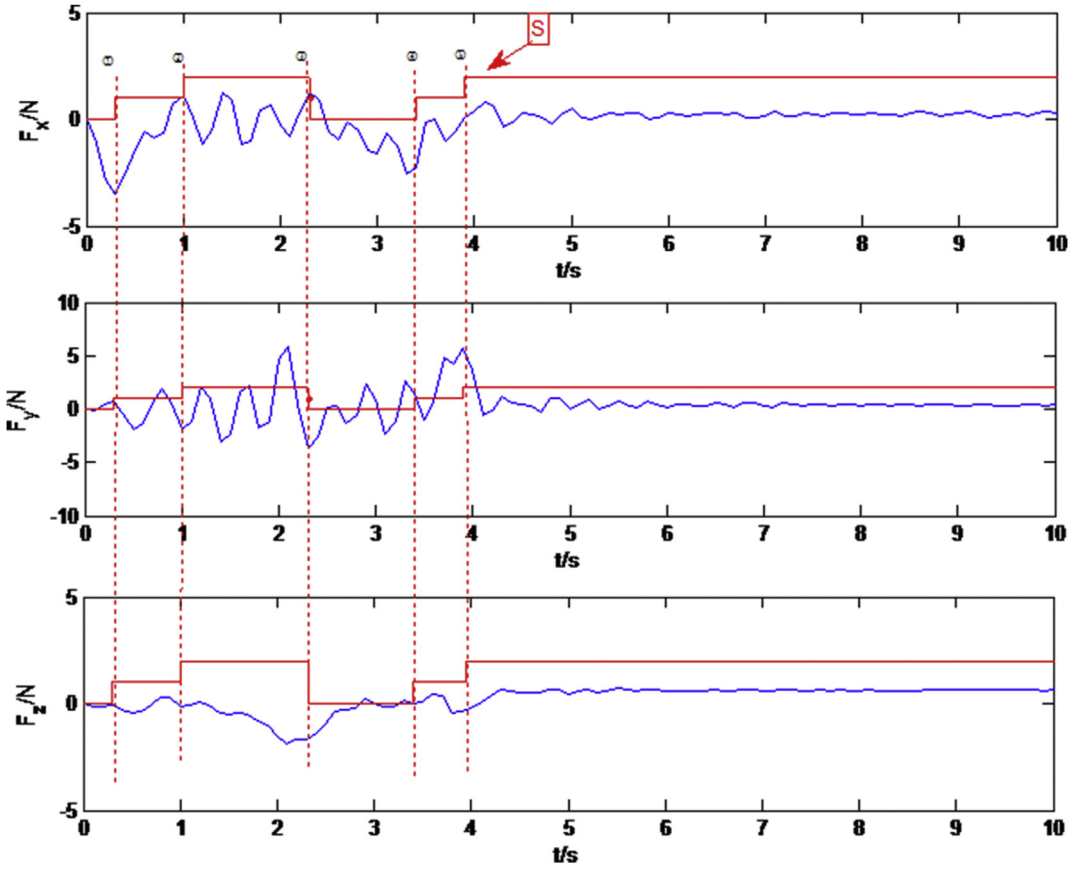

Fig. 8. Force response curve of Exp. II.

Through data analysis, as shown in Table 2 and Table 3, it should be noted that the average acting force in Experment I, II and III are almost the same. While the mean absolute deviations of Experiment I are bigger than that of Experiment II and III, especially the value on the Y-axis direction is twice bigger. In terms of torque, as shown in Figs. 7, 9 and 11, the mean value of Experiment I is about 10 times of the value of Experiment II and III. Experiment. A major drawback of Experiment I is that the force tendency can not be controlled. As shown in Fig. 6, the force in the X axis start to climb after 9 s. As it can be seen from the figure, Experiment III enter a stable state within 1 s. The response is quick, the force control is smooth and the operation is fast.

As shown in Fig. 8, in Experiment II, the solid line represents selection matrix S, the value represents the selected driving axis. It can be seen that S changed five times during the experiment. The initial driving axis is the X axis, which has a deviation of 45° with the door opening direction. Y axis is selected as the driving axis when the force on the X-axis exceeds the threshold at time ①. The driving axis is converted to Z-axis when the force acting on Y-axis exceeds the threshold too at time ②. Since derivation of the driving axis and the door opening direction in the first two circles is relatively large, resulting in a relatively large force error, the forces acting on the X, Y-axis were not adjusted to within the threshold when Z-axis is driving axis, which leading to the Z axis force is not stable in the threshold range and gradually exceed the threshold. X-axis become the driving axis again at time ③, and after another round of adjustment, Z-axis is seleted at time ⑤ and finally stabilized. It can be seen from Fig. 8, the proposed method can reduce the force to within the threshold, and make it stable.

As shown in Fig. 8, in Experiment II, the solid line represents selection matrix S, the value represents the selected driving axis. It can be seen that S changed five times during the experiment. The initial driving axis is the X axis, which has a deviation of 45° with the door opening direction. Y axis is selected as the driving axis when the force on the X-axis exceeds the threshold at time ①. The driving axis is converted to Z-axis when the force acting on Y-axis exceeds the threshold too at time ②. Since derivation of the driving axis and the door opening direction in the first two circles is relatively large, resulting in a relatively large force error, the forces acting on the X, Y-axis were not adjusted to within the threshold when Z-axis is driving axis, which leading to the Z axis force is not stable in the threshold range and gradually exceed the threshold. X-axis become the driving axis again at time ③, and after another round of adjustment, Z-axis is seleted at time ⑤ and finally stabilized. It can be seen from Fig. 8, the proposed method can reduce the force to within the threshold, and make it stable.

Based on Experiment II, linear velocity of the end-effector is regulated in Experiment III. As shown in Figs. 10 and 11, the driving axis enter a stable state at time ②, only after one

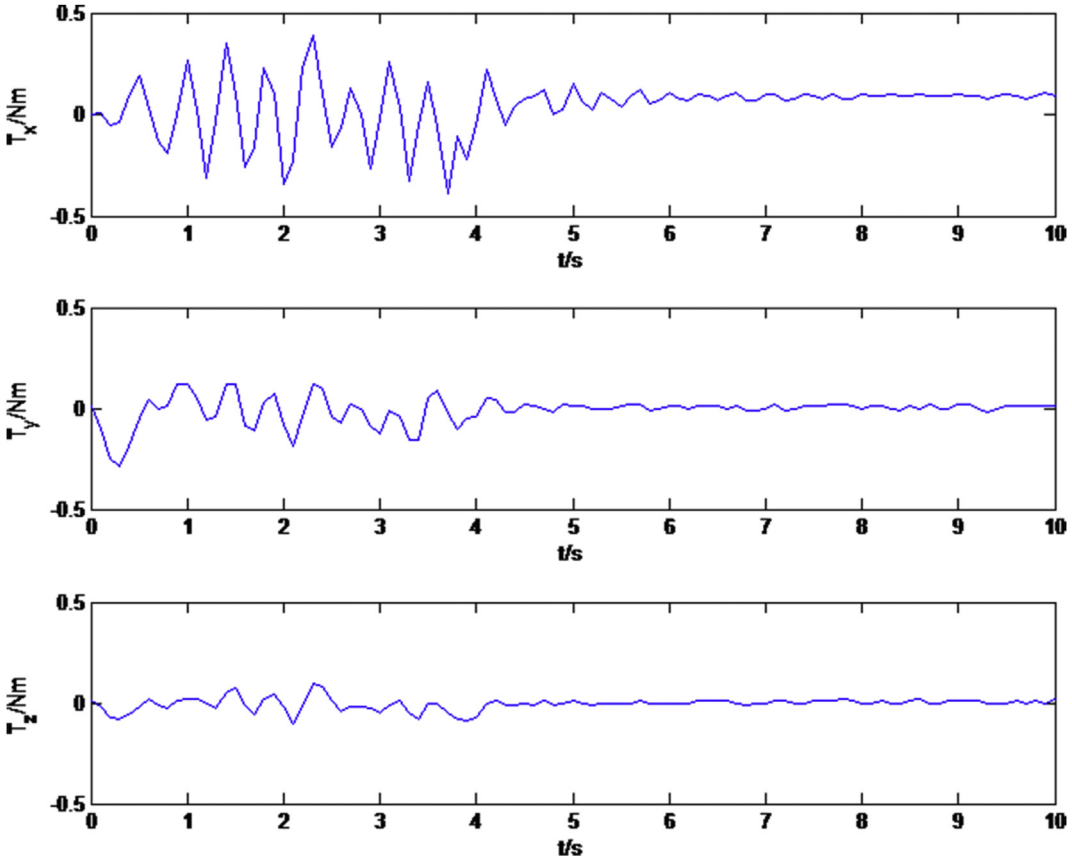

Fig. 9. Torque response curve of Exp. II.

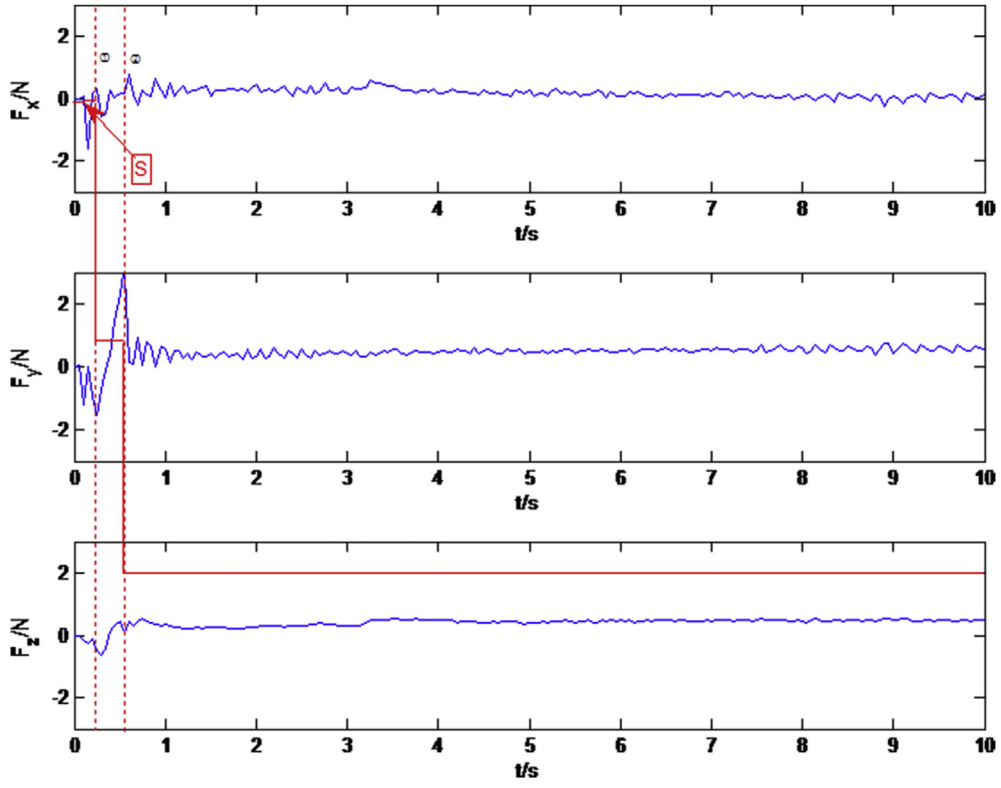

Fig. 10. Force response curve of Exp. III.

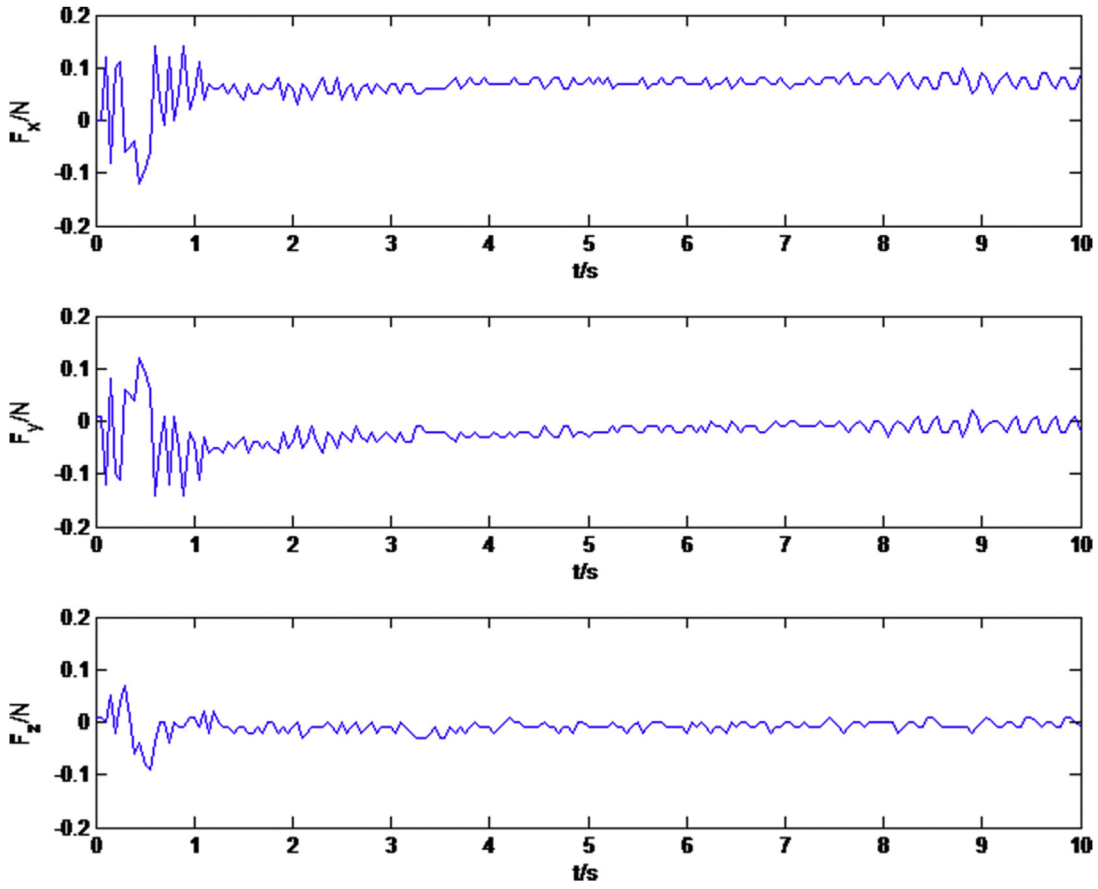

Fig. 11. Torque response curve of Exp. III.

selection period. The operation time for door open is shorter. The amplitude of linear velocity will change according to the variation of driving force dynamically. It will increase if the force decreases and it will decrease if the force increases, as shown in Fig. 12. When the deviation of the driving axis and the opening direction is not big, the force is relatively small, and the linear velocity is relatively large. It is possible to find the open direction faster because it will reduce the influence of the speed when adjusting the driving axis; When the deviation of the driving axis and the opening direction is big, the force is relatively big and the linear velocity is relatively small. It will be more smooth when adjusting driving axis. After entering the steady state, the amplitude of linear velocity increases to about 14 mm/s, and the door opening operation can be completed more quickly. The opening time in Experiment III is about 10 s, while they are about 17 s for Experiment I and Experiment II. As demonstrate in Experimental III, this method could reduce the overall time for door opening and improve the operation efficiency.

To verify the operation suitability of this method to different constrained mechanisms, experiment four and five experiments IV and V are conducted. The operation target of experiments IV is the door B. Dynamic resistance selection threshold γ is adopted here. The force response curve is shown in Fig. 13. As shown in Fig. 13, the selection matrix runs two cycles, the selection threshold was changed to 3N at time ①, so that the robot arm was adapted to the new unknown constrained mechanism. There is a peak force on Z-axis at time 3.5 s. this peak is considered as normal since it is within the threshold range. Eventually, the robot arm is able to operate door B continuously.

The operation target of Experiment V is a drawer, as shown in Fig. 5. The force response curve is plot in Fig. 14. Z axis is selected as the driving axis by selection matrix after one selection period, and the door opening task is successful completed. The suitability of this method to differenct constrained mechanisms is verified.

4. Conclusion

This paper proposed a Dynamic Interactive Control method to operate unknown constrained mechanisms. This method complete the task without the knowledge of the modeling of constrained mechanisms. In operation, on the one hand, the constraint coordinates will be estimated dynamically based on past speed directions, and the selection matrix will be adjusted online to decouple speed control and force control. On the other hand, in order to enhance the adaptability and interactivity of the operation task, the operating resistance and speed will be adjusted dynamically. Finally, the effectiveness and suitability have been verifed by experiments on constrained mechanism with different

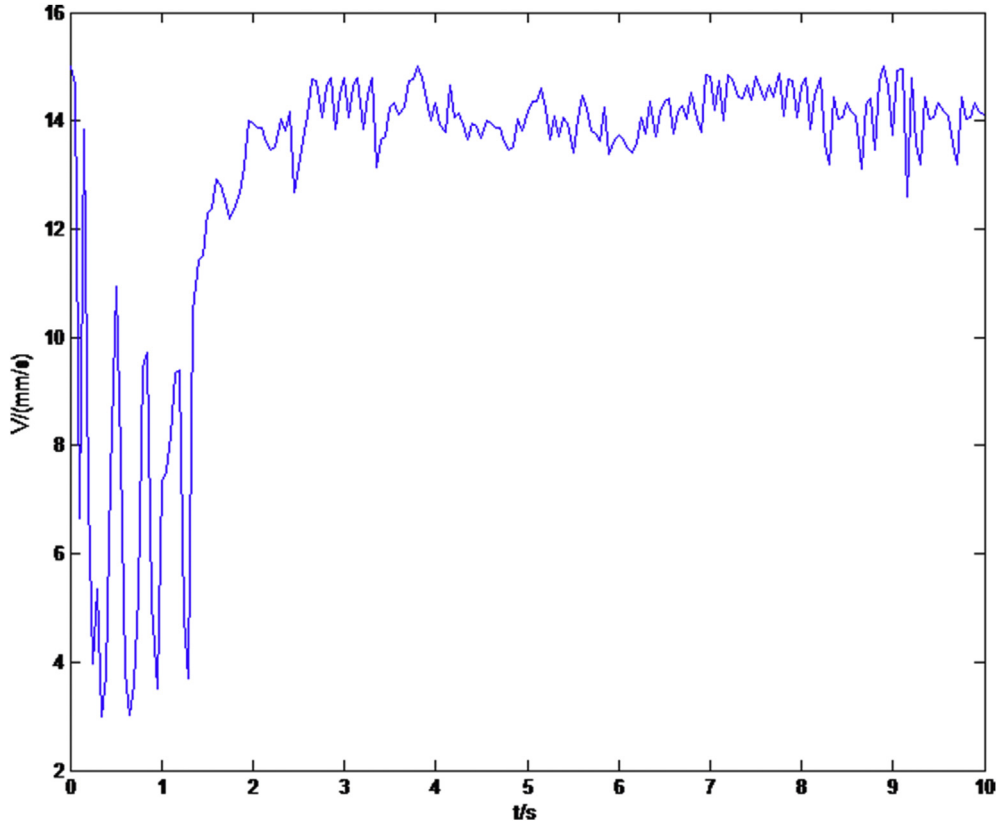

Fig. 12. The amplitude curve of velocity of Exp. III.

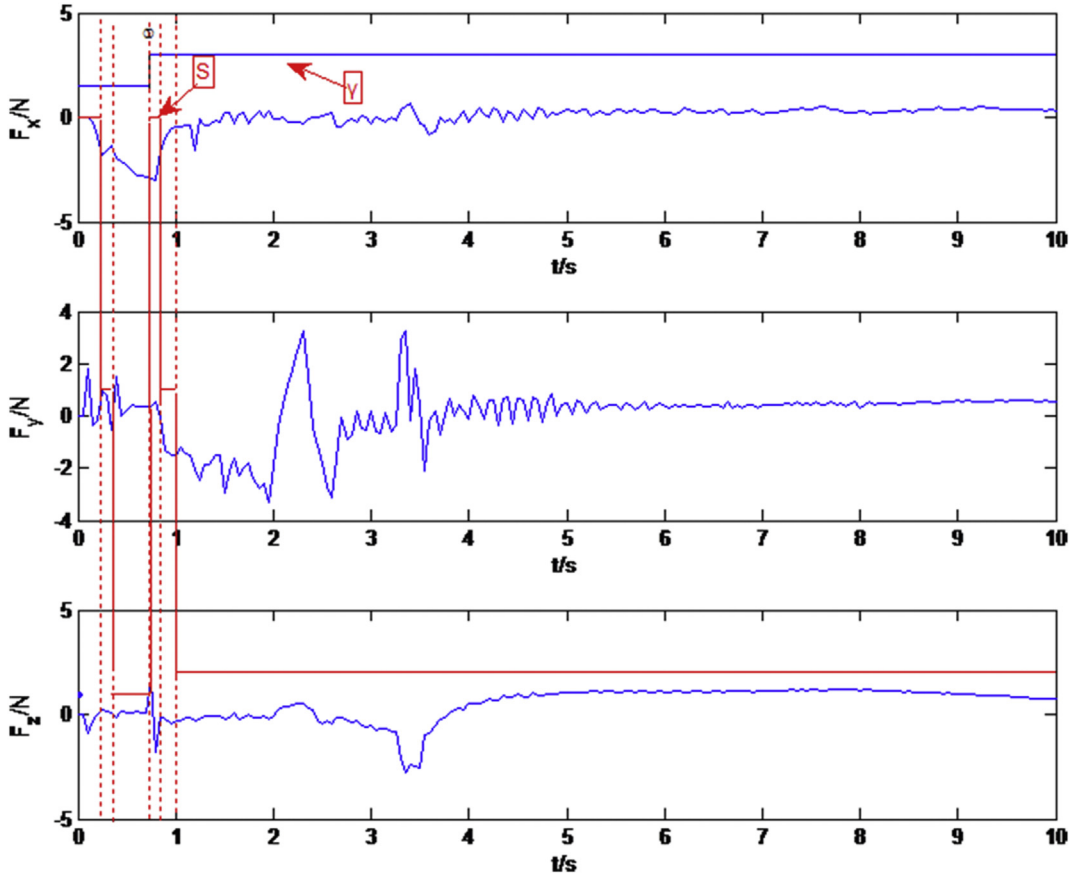

Fig. 13. Force response curve of Exp. IV.

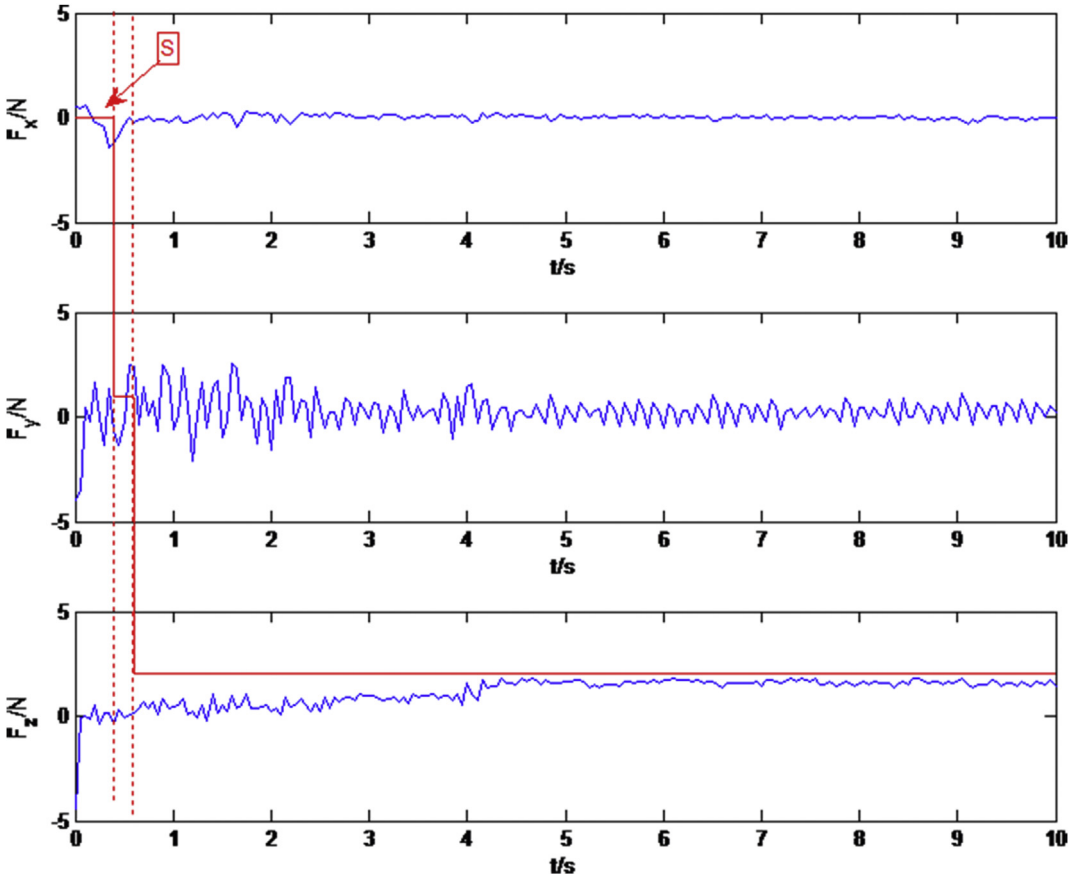

Fig. 14. Force response curve of Exp. V.

Table 2
The mean forces and their mean absolute deviations of Exp. I to Exp. III.

	X axis	Y axis	Z axis
Exp. I	0.0029	0.2350	0.4649
	0.1677	0.3242	0.1660
Exp. II	0.1799	0.7427	0.5247
	0.1586	0.1495	0.0879
Exp. III	0.0532	0.4051	0.6275
	0.1136	0.1660	0.1220

Table 3
The mean torques and their mean absolute deviations of Exp. I to Exp. III.

	X axis	Y axis	Z axis
Exp. I	0.0243	−0.0619	0.0844
	0.0314	0.0372	0.0460
Exp. II	0.0437	−0.0070	0.0008
	0.0098	0.0138	0.0088
Exp. III	0.0201	−0.0016	−0.0016
	0.0130	0.0101	0.0071

motion directions and resistance values. Currently, this method can only be applied to mechanism with only a single degree of freedom constrained motion. Future work will focus on how to extend this method to multi degree of freedom motion.

References

[1] M. Quigley, S. Batra, S. Gould, High-accuracy 3D sensing for mobile manipulation: improving object detection and door opening, in: IEEE International Conference on Robotics and Automation, Kobe Japan, 2009, pp. 2816–2822.
[2] G. Liu, S. Ahmad, L. Ren, Hybrid control of door-opening by modular re-configurable robots, in: IEEE/RSJ International Conference on Intelligent Robots and Systems, St. Louis, USA, 2009, pp. 954–959.
[3] M. Shimada, T. Asakura, Interactive manipulator interface with task planner, in: IEEE IECON 22nd International Conference on Industrial Electronics, Control, and Instrumentation, Taipei, 1996, pp. 481–486.
[4] K. Nagatani, S. Yuta, An experiment on opening-door-behavior by an autonomous mobile robot with a manipulator, in: IEEE/RSJ International Conference on Intelligent Robots and Systems, Pittsburgh, USA, 1995, pp. 45–50.
[5] K. Nagatani, S. Yuta, Designing strategy and implementation of mobile manipulator control system for opening door, in: IEEE International Conference on Robotics and Automation, Minneapolis, USA, 1996, pp. 2828–2834.
[6] L. Peterson, D. Austin, D. Kragic, High-level control of a mobile manipulator for door opening, in: IEEE/RSJ International Conference on Intelligent Robots and Systems, Takamatsu, Japan, 2000, pp. 2333–2338.
[7] A. Pujas, P. Dauchez, F. Pierrot, Hybrid position/force control: task description and control scheme determination for a real implementation, in: IEEE/RSJ International Conference on Intelligent Robots and Systems, YOKOHAMA, Japan, 1993, pp. 841–846.

[8] A. Petrovskaya, A.Y. Ng, Probabilistic mobile manipulation in dynamic environments, with application to opening doors, in: 20th International Joint Conference on Artificial Intelligence, Hyderabad, India, 2007, pp. 2178–2184.
[9] A.J. Schmid, N. Gorges, D. Goger, Opening a door with a humanoid robot using multi-sensory tactile feedback, in: IEEE International Conference on Robotics and Automation, Pasadena, USA, 2008, pp. 285–291.
[10] E. Lutscher, M. Lawitzky, G. Cheng, A control strategy for operating unknown constrained mechanisms, in: IEEE International Conference on Robotics and Automation, Anchorage. AK, USA, 2010, pp. 819–824.
[11] Y. Sun, W. Chen, Robotics 33 (5) (2011) 563–569 (in Chinese).
[12] D. Ma, H. Wang, W. Chen, Unknown constrained mechanisms operation based on dynamic hybrid compliance control, in: IEEE International Conference on Robotics and Biomimetics, Phuket, Thailand, 2011, pp. 2366–2371.
[13] M.H. Raibert, J.J. Craig, ASME J. Dyn. Syst. Meas. Control 103 (2) (1981) 126–133.
[14] N. Hogan, ASME J. Dyn. Syst. Meas. Control 107 (1) (1985) 1–25.
[15] W. Chen, Y. Sun, Y. Huang, Commun. Comput. Inf. Sci. 97 (1) (2010) 117–123.

Hesheng Wang (SM'2015) received the B.Eng. degree in Electrical Engineering from the Harbin Institute of Technology. Harbin, China, in 2002, the M.Phil. and Ph.D. degrees in Automation & Computer-Aided Engineering from the Chinese University of Hong Kong, Hong Kong, in 2004 and 2007, respectively. From 2007 to 2009, he was a Postdoctoral Fellow and Research Assistant in the Department of Mechanical and Automation Engineering, The Chinese University of Hong Kong. He has been with Shanghai Jiao Tong University, China, since 2009, where he is currently a Professor of Department of Automation. He worked as a visiting professor at University of Zurich in Switzerland. His research interests include visual servoing, service robot, robot control and computer vision. He is a senior member of IEEE. He is an associate editor of Robotics and Biomimetics, Assembly Automation, International Journal of Humanoid Robotics and IEEE Transactions on Robotics. He served as associate editor in Conference Editorial Board of IEEE Robotics and Automation Society from 2011 to 2015. Prof. Wang is actively involving in organization of international conferences. He served as organizing committee member for many international conferences such as ICRA and IROS. He was the general chair of the 2016 IEEE International Conference on Real-time Computing and Robotics and the program chair of the 2014 IEEE International Conference on Robotics and Biomimetic. He is the program chair of the 2019 IEEE/ASME International Conference on Advanced Intelligent Mechatronics.

Bohan Yang received the B.S. degrees in control engineering from Hunan University, Changsha, China, in 2014. She is currently working toward the M.S. degree in Department of Automation at Shanghai Jiao Tong University, Shanghai, China, since 2014. Her research interests include visual servoing, robot control and computer vision.

Weidong Chen received his B.S. and M.S. degrees in Control Engineering in 1990 and 1993, and Ph.D. degree in Mechatronics in 1996, respectively, all from the Harbin Institute of Technology, Harbin, China. Since 1996, he has been at the Shanghai Jiao Tong University where he is currently Head and Professor of the Department of Automation, and Director of the Institute of Robotics and Intelligent Processing. He is the founder of the Autonomous Robot Laboratory at the Shanghai Jiao Tong University. He was a visiting professor in the Artificial Intelligence Laboratory at the University of Zurich in Switzerland in 2012. He is a visiting professor in the Brain Science Life Support Research Center at the University of Electro-Communications in Japan from 2016 to 2017. Dr. Chen's current research interests include autonomous robotics, assistive robotics and medical robotics.